ISSN: 2754-4915

Journal of Material Sciences & Manufacturing Research

Research Article

Open Access

Contribution to the Understanding of Carbon Diffusion in Ferrite: Simulation Modelling

Growene W Queirós[2], Laura García[1*], Stefan Rafael Ruíz Delgado[1], J Victor Meseguer-Sanchez[3], José M Gómez de Salazar[3] and Antonio J Criado[1]

[1] Dpt. of Materials and Chemicals Engineering. Faculty of Chemistry, Complutense University of Madrid (U.C.M.), Madrid, Spain

[2] Dept. of Engineering, Faculty of Engineering and Technological Sciences, Rovuma University, Nampula, Mozambique

[3] Chair "Agringenia-Nutripeople, Circular Economy and RSD of the UCAM" UCAM University, Murcia, Spain

ABSTRACT

This research is focused on testing how the austenite breakthrough occurs in ferrite at a temperature of 850ºC. For this purpose, an experiment has been designed to deal with this fact at this temperature. A piece of F-114 steel was placed in contact with a piece of ARMCO iron. The F-114 steel at 850ºC transforms into austenite while the ARMCO iron remains as ferrite. The breakthrough takes place by slow diffusion of the carbon from the F-114 steel into the ferritic ARMCO iron matrix. This feed increases the carbon content of the ARMCO iron until it transforms it into austenite. The intimate contact between ARMCO iron and austenite has been carried out by hot forging without exceeding 850ºC. The metallographic study was carried out by scanning electron microscopy.

***Corresponding authors**

Laura García, Dpt. of Materials and Chemicals Engineering. Faculty of Chemistry, Complutense University of Madrid (U.C.M.), Madrid, Spain

E-mail: gslaura@quim.ucm.es

Received: June 23, 2022; **Accepted:** June 27, 2022; **Published:** June 30, 2022

Keywords: Ferrite, Steels, Diffusion, Metallography, Austenite

Introduction

We provide a practical and simple model for understanding how carbon diffusively moves into ferrite [1-14]. There has always been an attempt to understand the advancement of carbon in ferrite. We know that ferrite admits a very low carbon content in solution in ferrite, 0.008% by mass of carbon at room temperature and up to 0.028% by mass at temperatures of 720°C; which gives us an idea of the difficulties for carbon to circulate in the cubic lattice centered in the iron body in that temperature range, between 720°C and room temperature.

In order to observe the phenomenon at reasonable times, of this carbon circulating by diffusion in the network centered on the iron body, we have tried to accentuate this effect by carrying out the experiment at high temperatures without passing the ferrite-austenite transformation line, and thus always being in the ferritic field. The monitoring of the carbon diffusion is followed by the appearance of different morphologies of the iron carbide during cooling.

To achieve this, we have designed an experiment to keep the iron ferritic at the heating temperature, which has been 850ºC. To this end, the experiment was carried out with ARMCO iron, which is a high purity iron (C: 0.004%, Mn: 0.01%; P: 0.005% and S: 0.006%, by mass) [15]. The source of carbon is another steel, UNE F1114 steel (SAE 1040) whose composition is C: (0'40-0'45) %, Mn: (0'5-0'8) %; Si: (0'15-0'4) %, by mass.

UNE F1114 steel is fully austenitic at 850°C. The carbon diffuses fully into the γ phase of the iron, so it is necessary to put it in contact with the ARMCO iron and observe, after hours and days, how the carbon diffuses, using metallographic techniques to monitor the appearance of carbon by precipitation during the air cooling of the specimens.

The specimens are observed for diffusion into the ARMCO iron. The test times will vary according to the observation of the results.

Experimental Technique

The starting materials, ARMCO iron (C: 0'004%, Mn: 0'01%; P: 0'005% and S: 0'006%, by mass) and UNE F1114 (SAE 1040) steel (C: (0'40-0'45)%, Mn: (0'5-0'8)%; Si: (0'15- 0'4)%, by mass) were selected and the test specimens were machined.

A prismatic ARMCO iron specimen 50 mm long by 25 mm wide was made and a cylindrical specimen of UNE F1114 steel, 60 mm long by 10 mm in diameter, was inserted inside it. The assembly of the two steels is shown in figure 1.

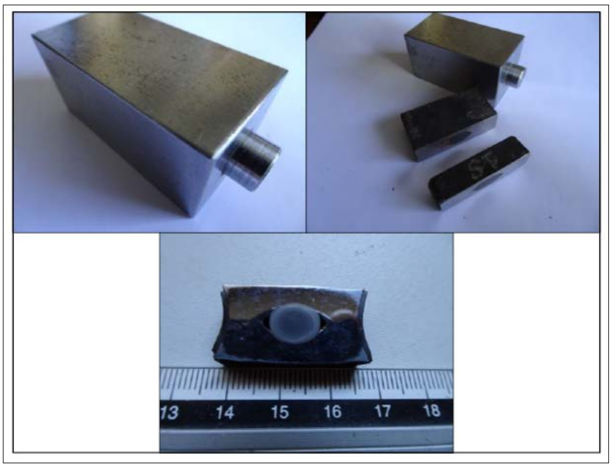

Figure 1: Initial Appearance of the Specimens Used

ARMCO iron has a microstructure consisting of ferrite grains, without any cementite or iron carbide crystals or any detectable impurities (Figure 2-3).

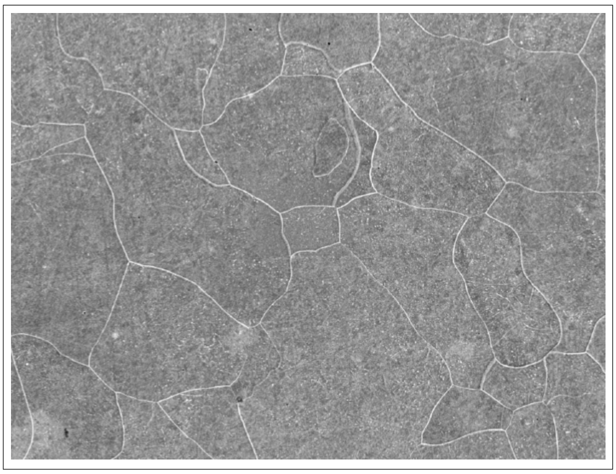

Figure 2: Microstructure of Armco Iron Showing Ferrite Grains With No Detectable Cementite Crystals, Iron Carbides or Impurities

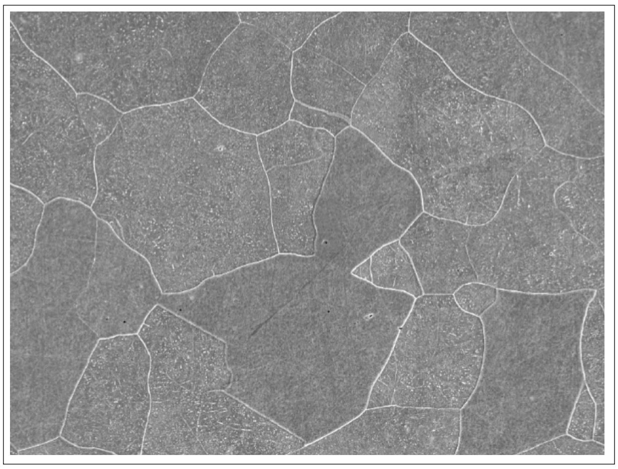

Figure 3: Detail, at Higher Magnification, of the Microstructure of Armco Iron Showing the Ferrite Grains Without Cementite Crystals, Iron Carbides or Detectable Impurities

The microstructure of UNE F-1114 steel consists of 50% pearlite and 50% ferrite, in equiaxial grains, very clean of any impurities (Figure 4-5).

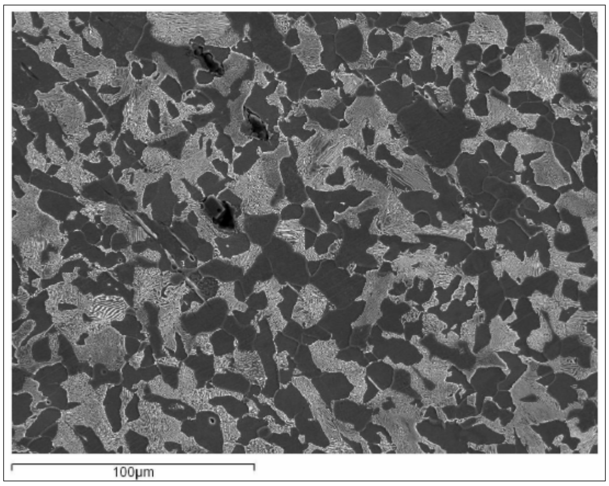

Figure 4: Microstructure of UNE F-1114 Steel Showing the Pearlite Lakes in a 50% Ferritic Matrix, Clean of Impurities

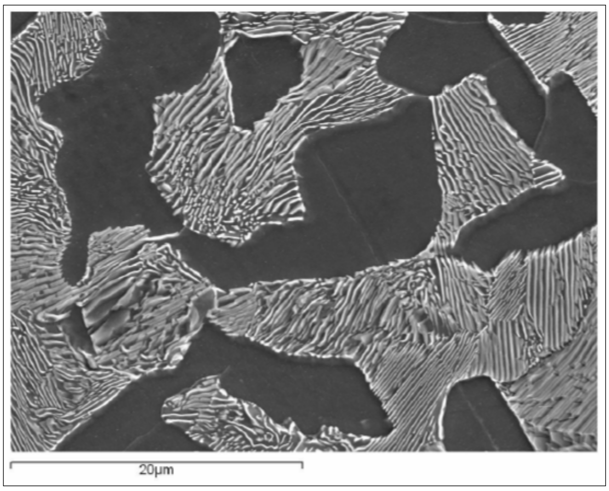

Figure 5: Detail of the Previous Microstructure of UNE F-1114 Steel

Once the assembly has been machined and assembled, with the two components as close together as possible, it was placed in a conventional electric furnace and heated to 850ºC, after which the assembly is laminated.

After reducing its geometry by approximately 20% of its thickness, it was left to cool. In this way, a perfect bond between the two materials is achieved, as can be seen in the micrographs in Figures 6 and 7.

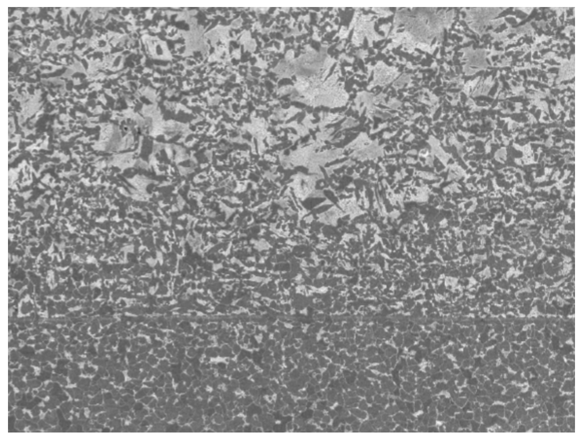

Figure 6: Microstructure Showing the Result of Joining the Two Steels

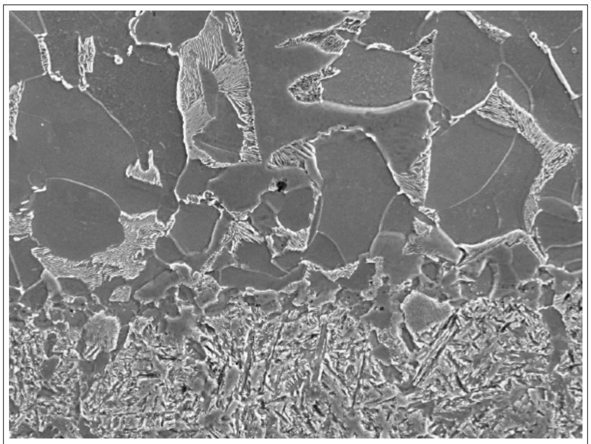

Figure 7: Detail of the Microstructure of the Previous Figure

Welding produces a forged joint in which, on the one hand, there is the high-carbon steel and, on the other hand, the ARMCO iron, with no carbon at all.

The welded assembly is then returned to the electric furnace and heated to a very controlled temperature of 850ºC and kept in these conditions for 7 days. After this time, specimens are cut from the part and prepared metallographically in the conventional way, by grinding with Buheler grinding paper of different grain sizes and subsequent polishing with 3µm and 1µm diamond paste. The specimens are then attacked with 2% Nital reagent for variable times of (30-60) seconds, in order to observe, metallographically by Scanning Electron Microscopy, in a JEOL JEM 3000F type microscope, how the different iron carbides and cementite appear.

Results

After 7 days of heating at 850ºC, the result of the carbon diffusion in the ferrite of the ARMCO iron can be observed. In figure 8, the micrograph obtained by SEM shows the diffusion advance fronts. A first boundary appears in the ARMCO iron, in the upper part where the advance of the carbon is observed with the appearance of small pearlitic colonies distributed in a ferritic mass of ARMCO iron, framed in the upper part by another boundary with the recrystallised grains of the ARMCO iron. The first border with the UNE F-1114 steel is very clearly visible and the second border, also very well marked, with the ferritic grains of ARMCO iron, still almost virgin, is perfectly drawn. Therefore, three zones are highlighted: the lower one with the UNE F-1114 steel, the second one in front with the advanced perlitic zone and the third one with the columnar grains of ARMCO iron.

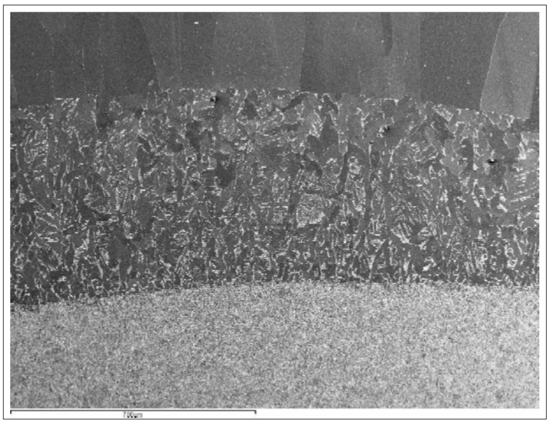

Figure 8: Microstructure of the sample part where the Carbon Diffusion Advance is Observed and Three Zones are Highlighted: The Lower One with the UNE F-1114 Steel, the Second One in Front with the Advanced Perlitic Zone and the Third One, in the Upper Part, with the ARMCO Iron Columnar Grains

Figures 9, 10 and 11, obtained by conventional optical microscopy, show these two borders and the three distinct zones mentioned above.

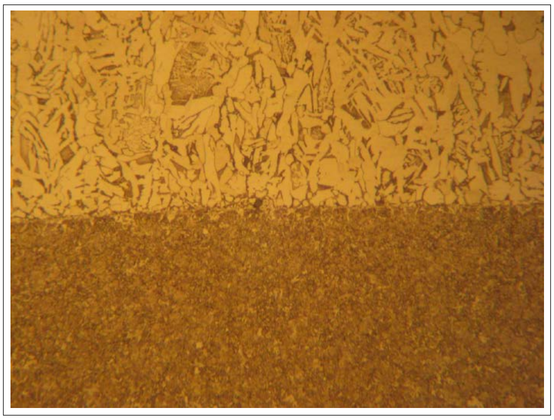

Figure 9: Microstructure, Obtained by Conventional Optical Microscopy, Showing the Border between the UNE F-1114 Steel (Lower) and the Advanced Perlitic Zone (Upper)

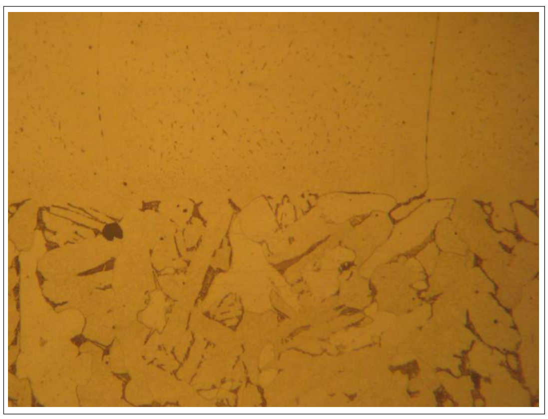

Figure 10: Microstructure, Obtained by Conventional Optical Microscopy, Showing the Advanced Perlitic Zone (Lower), with the ARMCO Iron Columnar Grains (Upper)

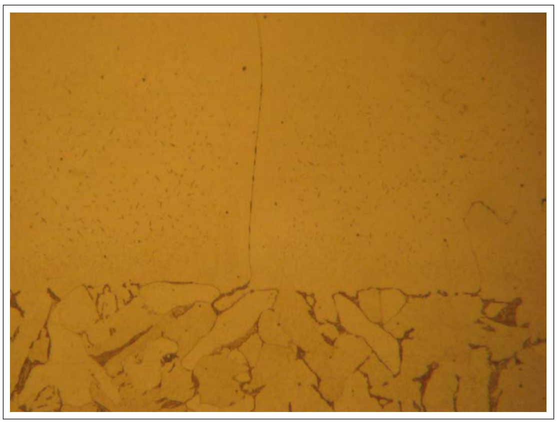

Figure 11: Detail of the Microstructure in the Previous Figure at Higher Magnification

The boundary marking the diffusion advance in ARMCO iron is clearly seen in figures 12 and 13. The structure of the columnar-grained ARMCO iron is seen bordering the equiaxial grains of diffusion-colonised ARMCO iron in the lower part of the micrograph. Figure 13, obtained by SEM, shows the structure of the intermediate zone, with small pearlitic colonies on ferritic grain boundaries recrystallised from ARMCO iron.

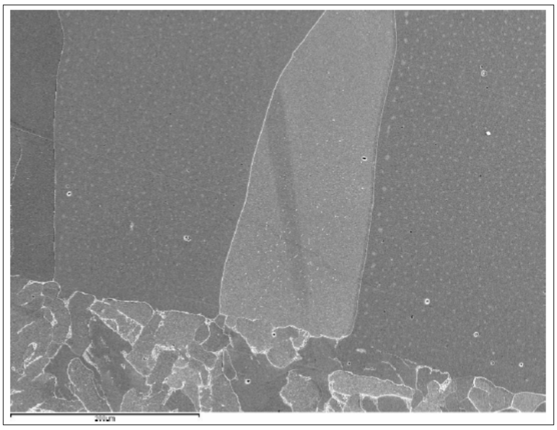

Figure 12: Microstructure, Obtained by Scanning Electron Microscopy, Showing the Advanced Perlitic Zone (Lower), with the ARMCO Iron Columnar Grains (Upper)

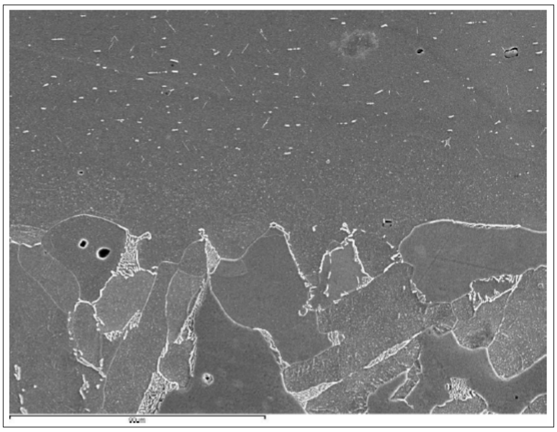

Figure 13: Microstructure, Obtained by Scanning Electron Microscopy, Showing the Boundary Between the UNE F-1114 Steel (Upper) and the Advanced Perlitic Zone (Lower)

Figures 14 to 19 show the initial carbon breakthrough in ARMCO iron in the form of small carbides precipitated during cooling. Sometimes across the grain boundary (figures 14 to 16) and sometimes more massively across grain boundaries and inside the ferritic grains of ARMCO iron (figures 17 to 20). Further into the interior of the ARMCO iron, there are no more traces to indicate whether there has been any diffusion. In the zone where the presence of carbon is already very scarce, at the advancing front, carbides with quasidendritic morphologies can be observed as shown in figure 20.

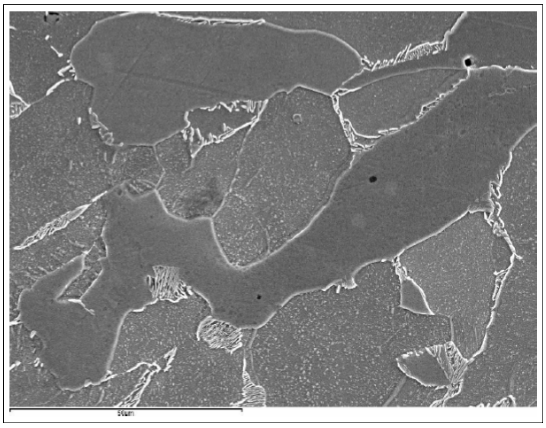

Figure 14: Microstructure, Obtained by Scanning Electron Microscopy, Showing the Advanced Pearlitic Zone

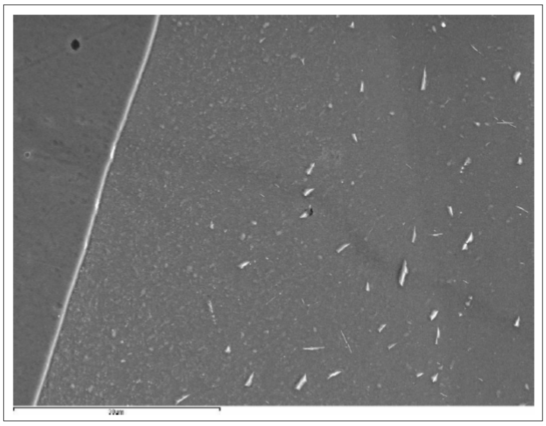

Figure 15: Microstructure, Obtained by Scanning Electron Microscopy, Showing the Columnar Grains of the ARMCO Steel

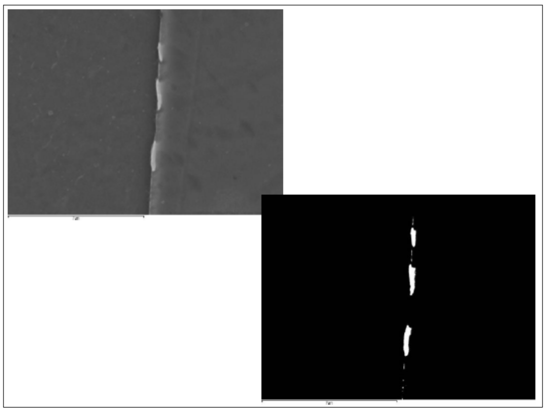

Figure 16: Microstructure, Obtained by Scanning Electron Microscopy, Showing Iron Carbides at the Grain Boundary, in the ARMCO Iron Columnar Grains

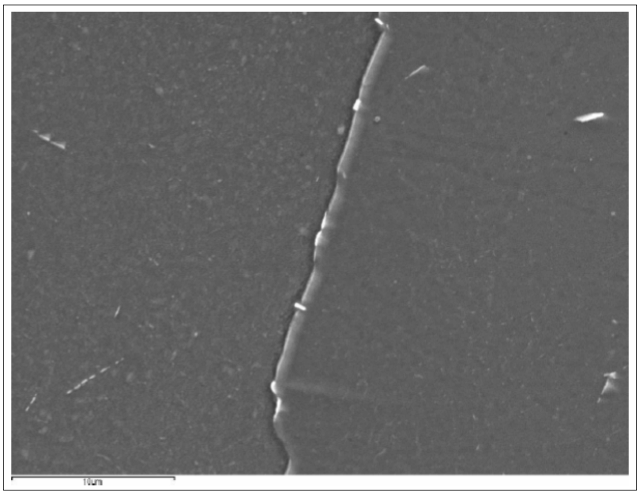

Figure 17: Microstructure, Obtained by Scanning Electron Microscopy, Showing a Detail of Figures 15 and 16

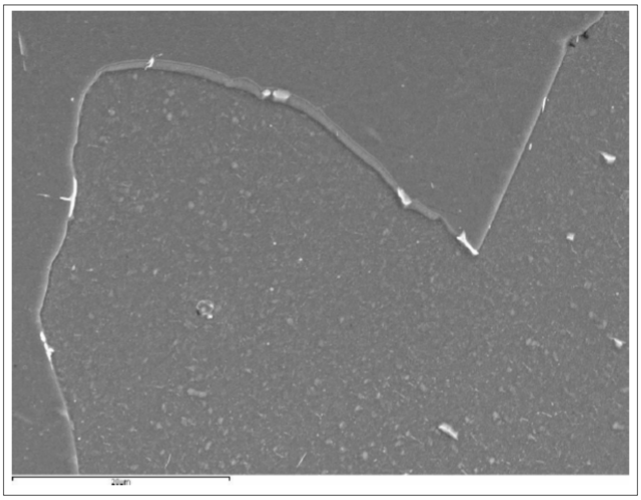

Figure 18: Microstructure, Obtained by Scanning Electron Microscopy, Showing Another Detail of the Iron Carbides at the Grain Boundary in the ARMCO Steel

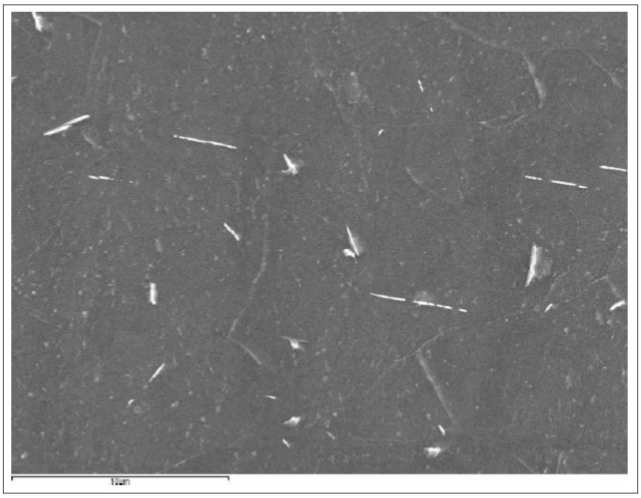

Figure 19: Microstructure, Obtained by Scanning Electron Microscopy, Showing Iron Carbides inside the ARMCO Iron Grain

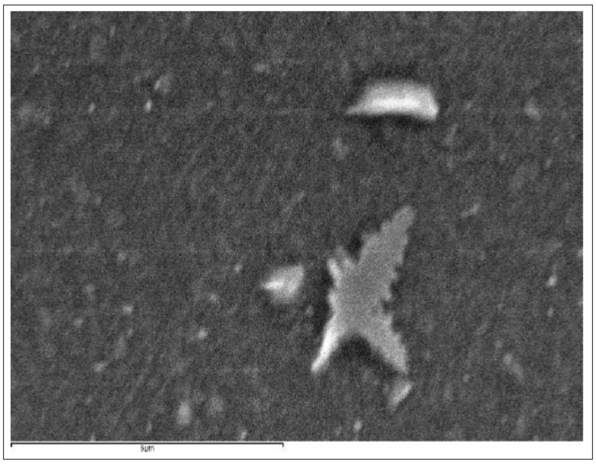

Figure 20: Microstructure, Obtained by Scanning Electron Microscopy, Showing a Stellate Iron Carbide inside the ARMCO Iron Grain

Conclusions

The aim of this study as can be seen in the experiment, the penetration of carbon through the ARMCO iron is very slow and difficult; in 7 days of heating, there is only slight carbon penetration, despite having been at 850ºC for that period of time. At lower temperatures, no apparent carbon diffusion is observed.

The slow diffusion of carbon into the ferrite at high temperatures takes place in distinct stages. The first is a small diffusion until the ARMCO iron ferrite increases in carbon content and forms austenite. Then, from this zone, carbon begins to diffuse in small quantities across the ferritic grain boundaries of the ARMCO iron and its matrix. This diffusion of ARMCO iron re-saturates the ferritic matrix and another stage of advancement into the ARMCO iron grains begins again.

This is a process very similar to that produced in the carburising of steels, although, as has been demonstrated, much slower, since the diffusion of carbon into ferrite is greatly impeded by the low solubility of this element in the ferritic, cubic crystal centred in the body.

References

1. Bhadeshia HKDH (1985) Diffusion formation of ferrite in iron and its alloys. Progressing Materials Science, Elservier 29: 321-386.
2. Aaronson HI, Reynolds WT Jr (1987) Further discussion to diffusional formation of ferrite in iron and its alloys. Scripta Metallurgical 21: 1611-1614.
3. Strangwood M (2012) Fundamentals of ferrite formation in steels. Phase Transformations in Steels, Elservier 1st Edition.
4. Ruda M, Farkas D, García G (2009) Atomist simulations in the Fe-C system. Computacional Materials Science 45: 550-560.
5. Hatcher N, Madsen GKH, Drautz R (2014) Parameterized electronic description of carbon cohesion in iron grain boudanies. J Phys Condens Matter 26: 1445502.
6. Oliveira FLG, Andrade MS, Cota AB (2007) Kiactics of austenite formation during continous heating in a low carbon steel. Material Characterization 58: 256-261.
7. Maucini R, Budde C (2002) Modelización de la reasterización en aceros Fe-C con difusidad de carbono dependiente de la concentración. Revista de Metalurgia 38: 426-432.
8. Pirz PA, Aristizabal RE, Serna CP (2018) Determination of

intercritical austenization parameters for development of multiphase steel using dilatometric analysis. Materia 23: e12044.
9. Yasara V, Luigi N (2011) Transformaciones de fase en aceros de bajo carbon. Rev Fac Ing UCV 26: 81-88.
10. Jiang DE, Carter EA (2003) Carbon dissolution and difussion in ferrite and austenite from first principles. Physical Review B 67:214103.
11. Nakahima K, Apel M, Steinbach I (2006) the role of carbón diffusion in ferrrite on the kinetics of cooperative grow of pearlite: a multi-phase field study. Acta Materialia, Elservier 54: 3665-3672.
12. Bhadeshia HKDH (1985) Diffusion- controlled growth of ferrite plates in plain-carbon steels. Materials Science and Technology 1: 497-504.
12. Veiga RGA, Becguart CS, Pérez M (2014) Atomistic modeling of a Fe-system with small concentration of C. Computacional Materials Science 82: 118-121.
13. Lugo N, Puchi ES, Cabrera JM, Pardo JM (2004) Deformación a velocidad variable de hierro ARMCO. Revista de Metalurgia 40: 139-145.
14. Liu YC, Sommer F, Mittemeijer FJ (2006) The austenite-ferrite transformation of ultralow carbon Fe-C alloys: transition from diffusion to interface controlled growth. Acta Materialia 54: 3383-3393.